

## Influence of borate amount on the swelling and rheological properties of the Scleroglucan/borax system

Tommasina Coviello,<sup>1</sup> Silvia Margheritelli,<sup>1</sup> Pietro Matricardi,<sup>1</sup> Chiara Di Meo,<sup>1</sup> Felice Cerreto,<sup>1</sup> Franco Alhauque,<sup>1</sup> Michela Abrami,<sup>2</sup> Mario Grassi<sup>3</sup>

<sup>1</sup>Dipartimento di Chimica e Tecnologie del Farmaco, Università di Roma "La Sapienza," Roma 00185, Italy

<sup>2</sup>Dipartimento di Scienze della Vita, Ospedale di Cattinara, Università di Trieste, Trieste I-34149, Italy

<sup>3</sup>Dipartimento di Ingegneria e Architettura, Università di Trieste, Trieste 34127, Italy

Correspondence to: T. Coviello (E-mail: tommasina.coviello@uniroma1.it)

**ABSTRACT:** Scleroglucan is a fungal polysaccharide that, when dispersed in water, assumes a very stable triple helix structure. It has numerous industrial applications in different fields, such as food industry, cosmetics, and pharmaceuticals. In the presence of borate ions, this polymer forms weak gels that, after freeze-drying and compaction, show an anisotropic swelling behavior, related to the borate/polymer ratio. By monitoring the evolution of the elastic and viscous moduli it was possible to follow the gel formation kinetics. The rheological properties of the network were studied as a function of crosslinking agent concentration and the corresponding flow curves and mechanical spectra were recorded. The kinetics of the crosslinking reaction was monitored by following the time evolution of the storage and loss moduli, after the addition of borate ions to the Scleroglucan system. Creep-recovery experiments allowed acquiring recoverable strain values and those of the critical stress above which a very high compliance of the sample is reached. Obtained results are to be related to the specific type of bonds between the polysaccharide chains and the crosslinking agent.

© 2015 Wiley Periodicals, Inc. *J. Appl. Polym. Sci.* **2016**, *133*, 42860.

**KEYWORDS:** gels; polysaccharides; rheology; swelling

Received 19 March 2015; accepted 18 August 2015

DOI: 10.1002/app.42860

### INTRODUCTION

Scleroglucan (ScIlg) is a neutral polysaccharide produced by fungi of the genus *Sclerotium* and its molecular structure is one of the stiffest found in nature. It dissolves in aqueous media as triple helix.<sup>1–3</sup> The polymer is very stable in a wide range of pH values and temperatures. The denaturation of the triple helix occurs only when the pH is higher than 13.5 or the temperature is increased up to 130°C. Because of its peculiar rheological properties and its resistance to hydrolysis, temperature, and electrolytes, ScIlg found various industrial applications (secondary oil recovery, ceramic glazes, food, paints, cosmetics, etc.) and it has been evaluated also for modified drug delivery systems.<sup>4,5</sup> In the presence of borate ions, ScIlg, like other polyhydroxylate polymers,<sup>6</sup> forms a weak gel: the diol groups of the side chains of the polymer can react with borate ions to give a di-ligand complex in which the borate ions act as “bridge-atoms” between the polysaccharidic chains thus forming a three-dimensional network.<sup>7</sup> Surprisingly, once freeze-dried and compressed, the obtained ScIlg-borax tablet shows a peculiar anisotropic elongation when soaked in aqueous media.<sup>8</sup>

Also other polymers, such as dextran, starch, pullulan, guar gum, locust bean gum, and polyvinyl alcohol can react with borax.<sup>9,10</sup> When soaked in a water medium, the tablets prepared with the corresponding systems showed the usual isotropic swelling with the exception of locust bean gum and guar gum. In particular, in the case of guar gum/borax tablets, an anisotropic swelling, similar to that of ScIlg/borax, was detected. Thus, the anisotropic elongation does not always occur and it cannot be considered as a general evidence. To explain this unusual behavior, it has been suggested that the borax-polysaccharides interaction takes place in different ways: in the case of guar gum, borax forms chemical bridges among the chains by means of reversible linkages while, in the case of ScIlg, borax promotes chemical and physical interactions between the triple helices.

In such system the formation of nanochannels was suggested and they were related to the alignment of triple helices that was mediated by the presence of borate ions.<sup>11</sup> Furthermore, by means of NMR studies, for the first time in a polysaccharidic hydrogel, an anomalous hyperdiffusive behavior of water molecules was detected.<sup>12</sup>

© 2015 Wiley Periodicals, Inc.

The ScI<sub>g</sub>/borax network, together with other ScI<sub>g</sub>-based systems, has been also extensively investigated as a potential carrier for modified drug delivery.<sup>13–20</sup>

The peculiar properties of ScI<sub>g</sub>/borax tablets, in terms of anisotropic swelling and anomalous water diffusion inside the network, in comparison to other polymeric systems, prompted us to investigate the effect of different amounts of borate ions on the rheological properties of the ScI<sub>g</sub>/borax system, in terms of flow curves and mechanical spectra. Creep-recovery experiments were also carried out and allowed to estimate the recoverable strain and the critical stress that defines the maximum value before the compliance of the system becomes very high. Furthermore, the effect of the presence of borax on the anisotropic elongation, when the gel was used for the preparation of tablets, was studied. The experimental data showed that the influence exerted by borax on the supramolecular structure of ScI<sub>g</sub>/borax system is related to the ratio ( $r$ ) between the moles of borax and the moles of ScI<sub>g</sub> repeating units. In addition, the kinetics of the network formation was followed by monitoring the time evolution of the storage and loss moduli after the addition of borate ions to ScI<sub>g</sub>.

## MATERIALS AND METHODS

Scleroglucan (Degussa, Germany;  $M_w = 1.1 \times 10^6$ , from viscometric measurements) was purified by dialysis against distilled water at 4°C, with dialysis membranes with a cut-off of 12,000–14,000, and then used after a freeze-drying process. Sodium tetraborate decahydrate, borax (ACS reagent  $\geq 99.5\%$ ), was a Sigma–Aldrich (Germany) product. Distilled water was always used.

### Hydrogel and Tablet Preparations

For the preparation of the hydrogels, an appropriate amount of polymer (about 200 mg for the swelling experiments and about 34 mg for the rheological analysis) was magnetically stirred in water for 24 h. Then, the calculated amount (i.e., moles of borax/moles of repeating units of polymer =  $r = 1$  for tablet samples, and  $0.02 \leq r \leq 10$  for the swelling tests) of a 0.1M borax solution was added, and the systems were left under magnetic stirring for 5 min. During salt addition, because of the self-buffering effect of borax, the pH value was constant (pH = 9.0).

The obtained samples (polymer concentration,  $c_p = 0.7\%$  (w/v)) were kept 2 days at 7°C for gel setting. For tablet preparation, the hydrogels were previously freeze-dried and then compressed using an IR die (Perkin-Elmer hydraulic press) and applying a force of 5.0 kN for 30 s.

The weight of the tablets was  $230 \pm 10$  mg; their diameter was  $13.0 \pm 0.1$  mm and the thickness was  $1.4 \pm 0.2$  mm.

For the rheological measurements the following procedure was carried out: the ScI<sub>g</sub>/borax samples were prepared into beakers with a diameter (45 mm) larger than the plate-plate geometry of the rheometer, and then were kept at 7°C for additional 48 h, for gel settling. To prepare a sample easy to manipulate and no so thick to invalidate the rheological measurements, the volume of the polymer solution was appropriately chosen, so that a hydrogel thickness in the range of 1.0–3.0 mm could be obtained.

### Water Uptake and Dimensional Increase Studies

The swelling of tablets was carried out by soaking the tablets in 200 mL of distilled water at 37°C. At fixed time intervals, the tablets were withdrawn, the excess of water removed with soft filter paper for 5 s, and then the corresponding thickness ( $h$ ) and diameter variations were determined by means of a screw gauge with an accuracy of  $\pm 0.1$  mm. At the same time, the weight ( $w$ ) changes were also monitored, by sample weighting. All analyses were performed on three replicate samples. Because tablet diameters did not increase significantly during the experiments, only the recorded mean values of the relative increase of weight and thickness ( $(w - w_0)/w_0$  and  $(h - h_0)/h_0$ ) were reported. In all cases, variations of the experimental values were below 10% of the mean.

### Rheological Measurements

The rheological characterization of the samples was performed by means of a controlled stress rheometer (Haake Rheo-Stress RS300) equipped with a water bath (Thermo Haake DC50). Two geometries were used: a cone-plate (Haake C60/1 Ti, cone diameter = 60 mm and cone = 1°; plate MP60 steel 8/8", diameter = 60 mm) for ScI<sub>g</sub> and for the hydrogel samples (Haake PP35/S; diameter = 35 mm), a grained plate-plate device, to reduce the extent of the wall slippage phenomena.<sup>21</sup> To perform the measurements, the hydrogel, with a thickness of 1.0–3.0 mm, was removed with the aid of a small spatula from the beaker where it was settled and laid with care on the lower plate of the rheometer. The upper plate was then lowered until it reached the hydrogel surface. Gap setting optimizations have been undertaken according to the procedure described elsewhere.<sup>22</sup> Samples were loaded at a fixed temperature of 25°C, and coated around their periphery with light silicone oil to minimize loss of water and left unperturbed for 15 min before measurements (constant temperature, 25°C). Such temperature was chosen to further reduce the solvent evaporation and, anyhow, it must be pointed out that the rheological properties of ScI<sub>g</sub> do not significantly change within the temperature range 25–37°C.<sup>2,23</sup> Rheological tests were performed under continuous shear conditions in the stress range  $0.1 < \tau < 100$  Pa, as well as under oscillatory shear conditions to individuate the extension of the linear viscoelastic regime (stress sweep tests at 1 Hz) and to determine the mechanical spectra (frequency sweep) in the frequency range 0.01–10 Hz at constant deformation of  $\gamma = 0.01$  (well within the linear viscoelastic range for all the studied samples).

The generalized Maxwell model<sup>21</sup> was used for the theoretical dependence of the elastic ( $G'$ ) and viscous ( $G''$ ) moduli on pulsation  $\omega = 2\pi f$  ( $f$  = solicitation frequency):

$$G' = \sum_{i=1}^n G_i \frac{(\lambda_i \omega)^2}{1 + (\lambda_i \omega)^2}; \quad G_i = \eta_i / \lambda_i \quad (1)$$

$$G'' = \sum_{i=1}^n G_i \frac{\omega \lambda_i}{1 + (\lambda_i \omega)^2}; \quad (2)$$

where  $n$  is the number of Maxwell elements considered while  $G_i$ ,  $\eta_i$ , and  $\lambda_i$  represent, respectively, the spring constant, the dashpot viscosity, and the relaxation time of the  $i$ th Maxwell element. The simultaneous fitting of eqs. (1) and (2) to

experimental  $G'$  and  $G''$  data was performed assuming<sup>2</sup> that relaxation times ( $\lambda_i$ ) were scaled by a factor 10. Hence, the parameters of the model are  $1 + n$  (i.e.,  $\lambda_1$  plus  $G_i$ ). Based on a statistical procedure,<sup>24</sup>  $n$  was selected in order to minimize the product  $\chi^2(1+n)$ , where  $\chi^2$  is the sum of the squared errors.  $G'$  and  $G''$  data represent the average of three experiments.

Assuming an affine tetra-functional network, the revised Flory's theory<sup>25,26</sup> enables the determination of polymeric network crosslink density  $\rho_x$  (defined as the moles of junctions between different polymeric chains per hydrogel unit volume):

$$\rho_x = G/RT \quad (3)$$

where  $R$  is the universal gas constant,  $T$  is the temperature, and  $G$  (shear modulus) can be computed as the sum of the elastic contributions ( $G_i$ ) related to each element of the generalized Maxwell model describing the hydrogel mechanical spectrum.<sup>27</sup> Equation (3) implicitly implies that the rheological characterization is performed on a gel that did not undergo neither swelling nor deswelling with respect to the crosslinking conditions.

The use of the Flory's theory for biopolymer gels, whose macromolecular characteristics are far from those exhibited by rubbers, has been repeatedly questioned. However, quite recent results showed that very stiff biopolymers can lead to networks which are suitably described by a purely entropic approach as postulated by Flory's theory.<sup>28</sup> Practically, this holds when small deformations are considered, i.e., in the linear viscoelastic region. The enthalpic contribution needs to be accounted for only when the nonlinear viscoelastic field is explored. As the mechanical characterization performed in the present article was carried out in the linear viscoelastic region, the entropic contribution prevails in the description of the Sclg network and the use of Flory's approach is reasonable.

Finally, the equivalent network theory<sup>29</sup> allows evaluating the average network mesh size  $\xi$ :

$$\xi = \sqrt[3]{6/\pi\rho_x N_A} \quad (4)$$

where  $N_A$  is the Avogadro number.

The creep–recovery experiments (25°C) were performed by applying a constant shear stress ( $\tau$ ) for 5 min and measuring the resulting changes in strain ( $\gamma$ ). Recovery after removal of stress was, then, monitored over a further period of 5 min. The values of the applied stress were increased systematically, from 0.01 to 10 Pa. Creep–recovery curves are reported as values of compliance ( $J = \gamma/\tau$ ). In the linear viscoelastic range, the experimental compliance data were interpreted by means of the relation coming from the generalized Maxwell model:<sup>21</sup>

$$J(t) = \left( \sum_{i=1}^n \frac{\lambda_i G_i}{t + \lambda_i} \right)^{-1} \quad (5)$$

### Scanning Electron Microscopy (SEM)

The SEM images were obtained using a FEI Quanta 400 FEG apparatus. Tablets of Sclg and of Sclg/borax samples ( $r = 1.0$ ), cut along the transversal direction, were fixed on a stainless stub using a double sided tape and examined under vacuum (50 Pa), with no need for the gold coating technique, at an

accelerating voltage of 15 kV. All images were acquired digitally using xTmicroscope Control software at 400× magnification.

## RESULTS AND DISCUSSION

### Water Uptake and Dimensional Increase Studies

It has been reported that an anomalous anisotropic elongation (i.e., an almost negligible increase in diameter dimensions and, correspondingly, a considerable increase in the axial direction) is observed<sup>8,10</sup> when tablets of Sclg/borax are soaked in aqueous media: such effect can not be detected with tablets prepared with the plain polymer and, in such case, the usual isotropic swelling is recorded (Figure 1).

This macroscopic change can be somehow visualized, also by recording SEM images on the cross section of tablets prepared with Sclg alone (Figure 2, left) and with Sclg/borax (Figure 2, right). The two micrographs show how the introduction of the crosslinker changes the internal morphological features. While the Sclg tablet shows an amorphous-like texture, the Sclg/borax tablet shows a highly ordered configuration of parallel, aligned bundle of polymeric chains that insist for a long distance, almost visible with naked-eye. The picture at the right side of Figure 2 represents an indication of the structure at molecular level that completely disappears in the absence of borax (left side). This peculiar difference between the morphology of the two samples has a remarkable effect at the macroscopic level: actually, when the tablets, prepared with the Sclg/borax freeze-dried sample, are soaked in aqueous media a striking different behavior is observed during the water uptake process (Figure 1).

The Sclg/borax hydrogels are previously freeze-dried in order to remove the solvent, thus obtaining dry systems suitable for the compression procedure. It is important to underline that the freeze-dried step does not perturb the microscopic arrangements of the polymeric chains, as below explained in details.

According to Tanaka's theory,<sup>30</sup> a gel system swells isotropically in all directions, regardless of its starting geometry. The anomalous behavior observed with the Sclg/borax tablets has to be ascribed to the existence, in solution, of domains with an intrinsic ordered structure, as also detected in the SEM images of Figure 2, and previously evidenced by an AFM analysis.<sup>11</sup> The triple helices of Sclg, in the presence of borate ions, show a parallel arrangement. They are held together, partially by a covalent linkage in the positions 4,6 of the side-chain glucose ring<sup>17</sup> (as also evidenced by IR spectra<sup>8</sup>), and partially by physical interactions. The diol groups of the side chains of the polymer can react with borate ions leading to a di-ligand complex in which the borate ions act as “bridge-atoms” between the polysaccharidic chains. Thus, the obtained hydrogel can be identified as a “mixed” gel whose network is built up by means of both physical and chemical interactions between the polymer and the crosslinker. Furthermore, in the presence of a mechanical perturbation, given in the present case by the compression step, these ordered domains are being enhanced, leading to an asymmetrical disposition of the triple helices along a preferentially oriented direction. Thus, the “mixed” gel shows a fine balance between different effects: a particularly relevant swelling, not allowed in “pure” chemical gels, and, at the same time, the

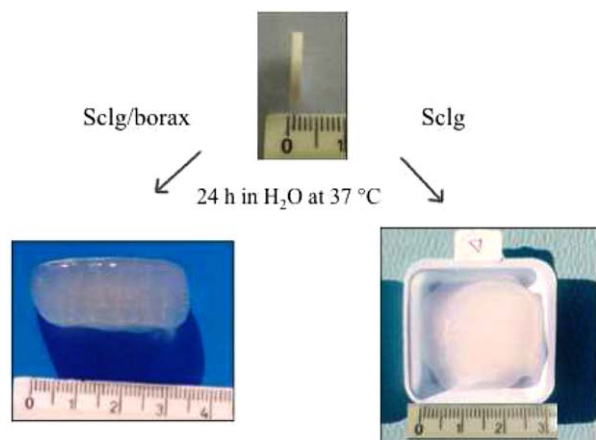


**Figure 1.** Swelling (distilled water, 37°C) of Sclg tablets prepared in the presence of (left), or without borax (right). [Color figure can be viewed in the online issue, which is available at [wileyonlinelibrary.com](http://wileyonlinelibrary.com).]

maintenance of the order present in the tablet, leading finally to the observed unusual anisotropic swelling. It has been suggested that the addition of borax to Sclg leads to the formation of oriented soft nanochannels (according to MD simulations).<sup>11</sup> These channels may trap water molecules and force them to move randomly along the nanochannel directions. By NMR experiments a superdiffusive regime has been detected in the Sclg/borax system, while this behavior disappears in the direction perpendicular to the tablet compression, thus suggesting the specific role of the structure and orientation of the soft nanochannels in the gel.<sup>12</sup> It was suggested that the compression of Sclg/borax tablets modify the orientation of the nanochannels in such a way that the system behaves as a strong adsorber along the direction of compression and a weak adsorber in the perpendicular direction. This model can explain the preferential orientation of the nanochannels along the compression direction.

The relative weight increase of tablets, prepared with the freeze-dried hydrogel of Sclg/borax with different  $r$  values (0.02, 0.05, 0.12, 0.25, 0.50, 1, 2, 3, 4, 7, 10), was monitored after immer-

sion in distilled water at 37°C. In addition, the relative increase of tablet height,  $h$  (axial direction), was recorded. Results, reported in Figure 3, clearly show that the water uptake was deeply dependent on the  $r$  value.

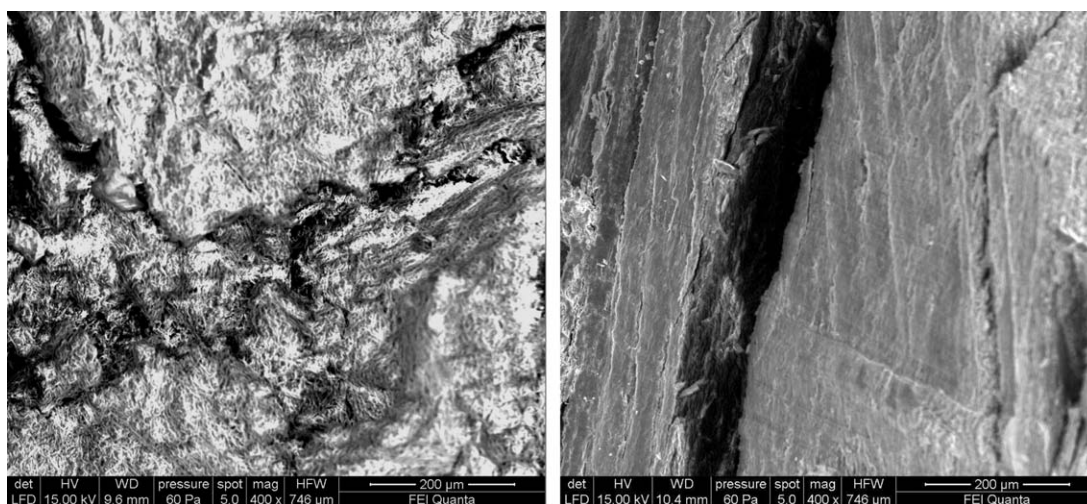
From the data reported in Figure 3(A,B) it is evident how the samples with the lowest amount of borax ( $r=0.02$  and  $0.05$ ) showed the weight increase and the asymmetric elongation reduced to  $\sim 50\%$  in comparison with the sample characterized by  $r=1$ , chosen as the reference system.

Systems characterized by  $r=0.12$ ,  $0.25$ , and  $0.50$  showed a behavior super-imposable to that of the  $r=1$  system. The experimental data for the systems characterized by  $r \geq 1$  are displayed in Figure 3(C,D). As the amount of borax increases, a corresponding decrease in the water uptake and in the elongation occurred. In Figure 4 the data of all samples, evaluated after 8 and 24 h, are reported on a logarithmic scale.

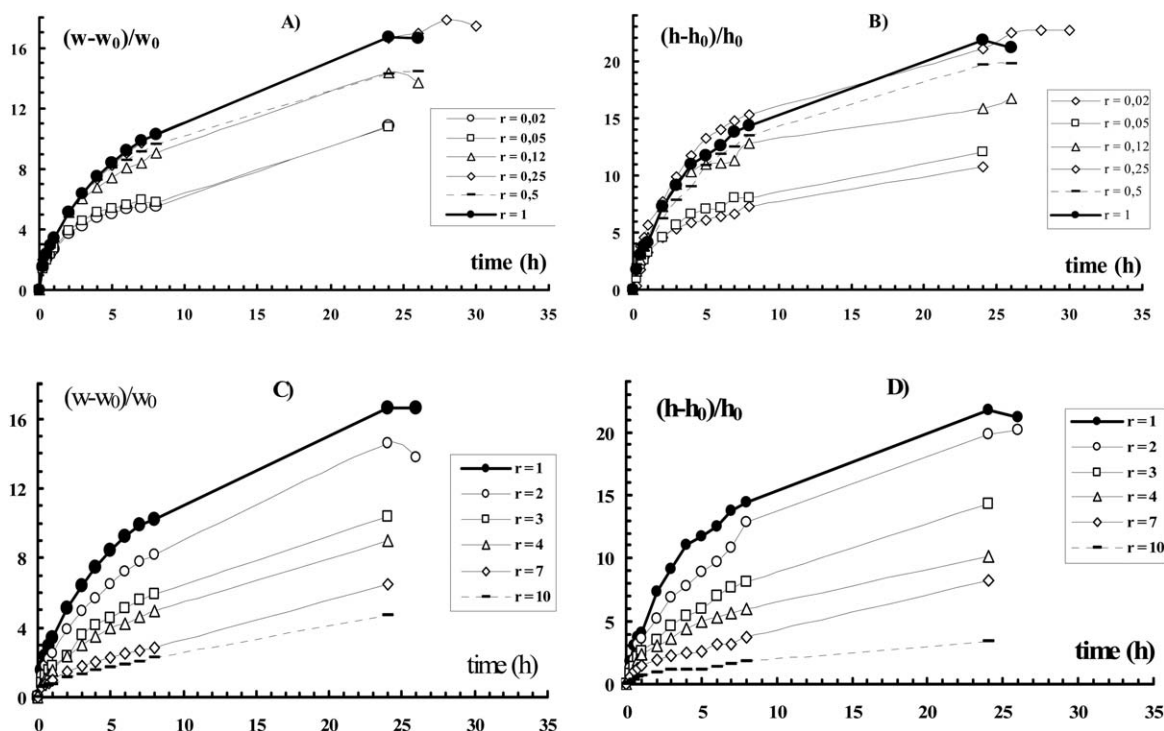
It is worth to note that, for  $r$  values between  $0.25$  and  $2$ , almost constant values for the relative water uptake and height increase were observed. Thus, it can be asserted that a quite small amount of borax ( $r=0.25$ ) is already capable to promote the asymmetric elongation that shows similar values up to  $r=2$ . On the other side, higher amounts of borax ( $r > 2$ ), induce a significant reduction in both, water uptake and asymmetric elongation. In particular, for  $r \geq 2$ , water uptake and elongation follow a power law reduction, indicating the strong relation between the presence of borax and the imbibition process of the matrices. These evidences lead to the conclusions that an excess of borax ( $r > 2$ ) significantly disturbs the matrix swelling, dramatically reducing solvent uptake and matrix elongation. It can be stated that the dependence on borate ions is stronger for the anisotropic elongation than for the water uptake.

#### Rheological Studies

Figure 5, showing the stress sweep tests for systems characterized by  $r=0$ ,  $0.12$ ,  $2$ , and  $7$ , evidences that  $G'$  is always prevailing on  $G''$  and both of them are independent from the deformation  $\gamma$  up to the critical value,  $\gamma_c$ , indicating the limit of the linear viscoelastic region. It is interesting to point out that



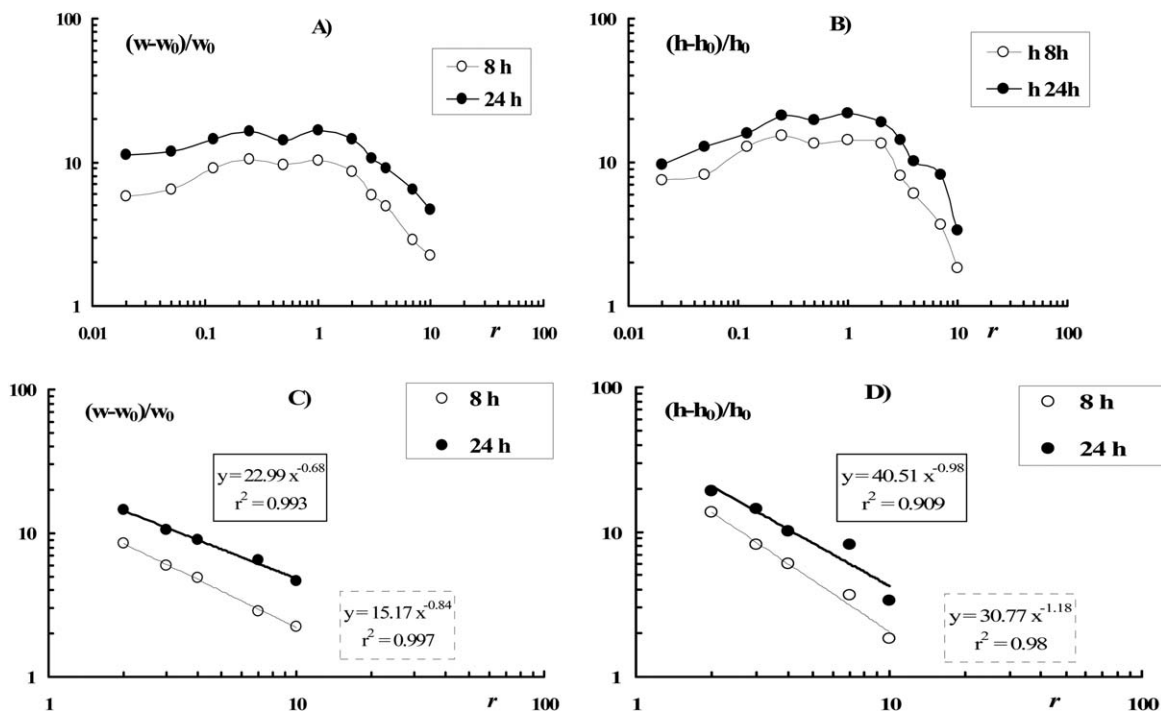
**Figure 2.** SEM images of tablet cross-sections. Left: Sclg tablet; right: Sclg/borax tablet (magnification =  $400\times$ ,  $c_p = 0.7$ ,  $r = 1$ ).



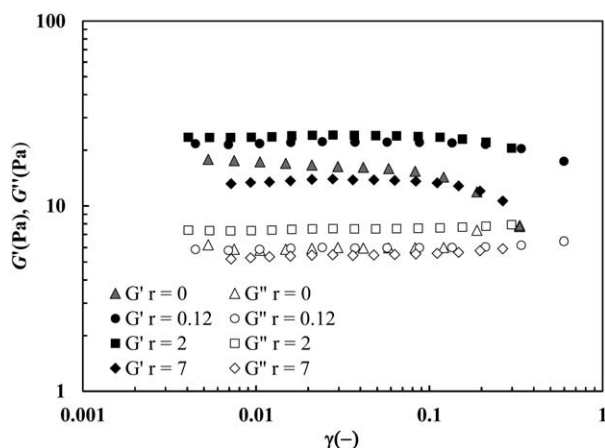
**Figure 3.** Relative increase of the weight,  $w$  (A and C), and height,  $h$  (B and D), for ScIg/borax tablets prepared with different  $r$  values, as a function of time (swelling medium: water at 37°C). Solid lines are only a guide to the eye. A and B: tablets with  $r \leq 1$ ; C and D: tablets with  $r \geq 1$ .

Table I indicates that  $\gamma_c$  (and  $\tau_c$  critical stress) tends to increase with  $r$  up to  $r = 1$  and then it goes back to the value assumed for  $r = 0$  (ScIg alone). This means that, up to  $r = 1$ , the presence of borax implies an increase of the system's strength due to

inter-chains crosslinking. On the other side, a further  $r$  increase implies a system weakening as shown by both Figure 5 and Table I. Further insight about the rheological properties of the studied systems can be gained by the evaluation of Figure 6 and



**Figure 4.** Relative increase of the weight (A) and height (B), after 8 and 24 h, for ScIg/borax tablets prepared with different  $r$  values, as a function of time (swelling medium: water at 37°C). Solid lines are only a guide to the eye. A and B: all tested samples; C and D: data for tablets with  $r \geq 2$ .



**Figure 5.** Stress sweep tests for systems characterized by different values of  $r$ . For the sake of clarity, only some of the studied systems are reported.  $\gamma$  is the deformation while  $G'$  and  $G''$  are the storage (or elastic) and the loss (or viscous) moduli, respectively.

Table II that show the results of the frequency sweep tests referring to the studied systems.

A deeper insight of Figure 6 and Table II shows that the systems with  $0.12 \leq r \leq 4$  behave as weak gels, as  $G'$  is clearly prevailing over  $G''$  within the whole  $\omega$  field explored, both moduli are parallel but they show a moderate decrease as  $\omega$  decreases. On the other side for  $r=0$  and  $r=7$ , although  $G'$  always exceeds  $G''$ , both moduli are clearly dependent on  $\omega$  and the crossover point seems to appear just after the lowest investigated  $\omega$  value. Accordingly, these systems represent a sort of transient system between a solution and a weak gel. These considerations are supported by the value of the average complex modulus  $\overline{G^*}$ , computed resorting to the average storage ( $\overline{G'}$ ) and loss ( $\overline{G''}$ ) modulus evaluated on the explored pulsation ( $\omega$ ) field. Indeed,  $\overline{G^*}$  is clearly smaller for the  $r=0$  and  $r=7$  systems (see Table II). Thus, for  $0.12 \leq r \leq 4$  it is reasonable to suppose that the presence of borate ions leads to a fully developed three-dimensional polymeric network; while an excess of borate ions ( $r=7$ ) seems to hinder the formation of a fully structured polymeric network. It is interesting to note that the network formation requires a very small amount of borax ( $r=0.12$ ) and a further addition of borate ions does not significantly affect the gel strength ( $\overline{G^*}$ ). Nevertheless, we can see a gel strength increase up to  $r=1$ , followed by a decrease up to  $r=4$ . A further support to this interpretation is given by the swelling experiments (Figure 4) that show an almost constant weight and height increase of the systems for  $0.12 \leq r \leq 4$ , while a clear decrease is observed for  $r < 0.12$  and  $r > 4$ . Indeed, it is reasonable that, for a given polymer, a fully developed polymeric network can show a higher swelling degree than that of a not completely, or partially, developed one.

**Table I.** Critical Deformation ( $\gamma_c$ ) and Stress ( $\tau_c$ ) for Systems Characterized by Different  $r$  Values

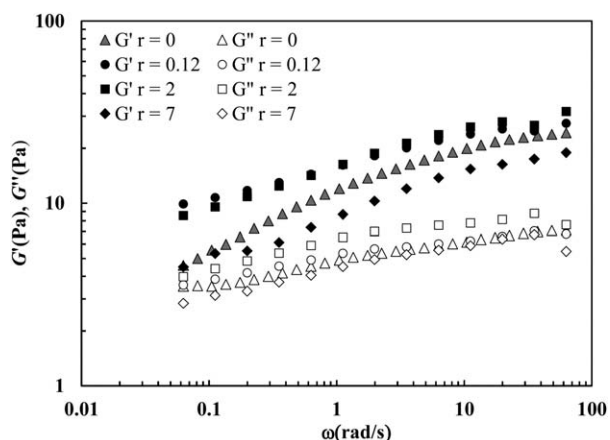
$r(-) =$	0	0.12	0.5	1	2	4	7
$\gamma_c(-) =$	0.082	0.135	0.216	0.300	0.212	0.149	0.083
$\tau_c(\text{Pa}) =$	1.4	3.0	5.0	8.00	5.0	2.8	1.2

Table II shows that, for almost all  $r$  values, five Maxwell elements are required for a satisfactory data fitting (see  $F$  test). The only exception is represented by the case  $r=7$  where only four Maxwell elements are necessary. Based on these results, it was possible to evaluate the shear modulus  $G$  for all systems, as reported in Table II. Equations (3) and (4) allowed the estimation of the crosslink density ( $\rho_x$ ) and the average mesh size  $\xi$  (see Table II). The small  $G$  values are related to the small  $\rho_x$  values and, consequently, to big mesh sizes for all systems. As  $\xi$  is statistically equal for systems characterized by  $0 \leq r < 7$ , it can be stated that the effect of borate ions does not induce modifications of the polymeric network architecture. From a rheological point of view, the borate ions simply strengthen the polymeric network by reinforcing the crosslinks that, in the case of ScI<sub>g</sub> alone, are only due to physical and topological reasons, without inducing dramatic changes in the moduli values.

Most striking is the effect of the crosslinker in the ScI<sub>g</sub>/borax tablets. In fact, as above reported, at the beginning the diol groups of the side chains of the polymer can react with the borate ions to give a di-ligand complex in which the ions act as “bridge” among the polysaccharidic chains. Bundles of such kind of chains form domains with an intrinsic ordered structure that, in the presence of a mechanical perturbation (compression step) is remarkably enhanced and leads to an asymmetrical disposition of the helices along a preferentially oriented direction.<sup>7,11</sup>

However, in the case  $r=7$ , the large excess of borate ions weakens the crosslinks strength and this leads to the formation of a quite large mesh size of the network (see Table II). In fact, the electrostatic repulsion among the helices, due to the presence of a high amount of borax, hinders the formation of “bridges” among the polymeric chains and the borate ions.

Rheology can also provide interesting information about the kinetics of gel formation after the addition of borate ions. Indeed the crosslinking process is not instantaneous as the addition of borax to ScI<sub>g</sub> is usually followed by a lag time of 2 days for a complete gel setting. Accordingly, network formation was followed by monitoring the time evolution of  $G'$  and  $G''$  at the frequency of 1 Hz and 25°C. The results of this test are shown in Figure 7(A) where it is possible to observe that  $G'$  increases within the first 4–5 h and then it becomes almost constant. At the same time the loss modulus  $G''$  does not show any significant change, being the viscous component not appreciably affected by the presence of borax. This effect is clearly seen also in Figure 7(B), showing the mechanical spectra recorded just after borate ions addition ( $t=0$ ) and after  $t=20$  h. While for  $t=0$  an almost liquid-like behavior is observed, as  $G'$  and  $G''$  depend on pulsation and  $G'$  decreases more rapidly than  $G''$  at lower  $\omega$  values (the crossover point seems to be very close to



**Figure 6.** Frequency sweep tests for systems characterized by different  $r$  values. For the sake of clarity, only some of the studied systems are reported.  $\omega$  ( $= 2\pi f$ ,  $f$  is the solicitation frequency) is the pulsation while  $G'$  and  $G''$  are, respectively, the storage (or elastic) and the loss (or viscous) moduli.

the lowest  $\omega$  considered), for  $t = 20$  h,  $G'$  is always about 10 times  $G''$  and the decrease of both  $G'$  and  $G''$ , as  $\omega$  decreases, is significantly lower. In addition,  $G'$  and  $G''$  are parallel.

The creep-recovery curves were recorded, at 25°C, for the ScIlg sample ( $c_p = 0.7\%$ ) and for the hydrogels ScIlg/borax characterized by  $r = 0.12, 1, \text{ and } 7$  ( $c_p = 0.7\%$ ). The system with  $r = 0.12$  was selected since the elongation of the corresponding tablets was almost superimposed to that of the tablets prepared with  $r = 1$ . The sample with  $r = 7$  was chosen because the tablets prepared with such hydrogel showed a significant reduction in the anisotropic elongation, in comparison to that of the tablets prepared with ScIlg/borax  $r = 1$ , taken as the reference system. Furthermore, for an appropriate comparison, also the creep-recovery curve of the polymer without borax ( $r = 0$ ) was carried out. To establish a

link between the creep and the frequency sweep tests, the stress ( $\tau$ ) imposed in the creep-recovery test was set at 0.1 Pa. Thus, the maximum deformation reached in the creep phase never exceeded the critical deformation  $\gamma_c$  which represents the upper limit of the linear viscoelastic range (see Table I). Figure 8(A) clearly underlines the good fitting of eq. (5) to the experimental data (see also  $F$  test reported in Table III) for all the considered systems ( $r = 0, 0.12, 1, \text{ and } 7$ ). Fitting results, in terms of  $G_i$  and  $\lambda_1$ , are reported in Table III. The comparison of these results with those obtained by the fitting [eqs. (1) and (2)] of frequency sweep data (see Table I) confirms the agreement of the two approaches. Indeed, it can be seen that the order of magnitude of the shear modulus ( $G$ ) is, approximately, the same for the two approaches. The maximum difference (62%) occurs for the  $r = 0.12$  system. As an example, Figure 8(B) shows the comparison between the relaxation spectra ( $G_i$  and  $\lambda_i$ ), calculated according to eqs. (1) and (2) (filled symbols), and those obtained from eq. (5) by fitting the experimental data (open symbols). It can be observed that, although five Maxwell elements are needed according to eqs. (1) and (2) fitting, and only four elements are required by eq. (5) fitting, the shape of the relaxation spectrum is similar (also taking into account the standard deviation related to each parameter in the  $x$  and  $y$  direction). The most important difference arising between the two spectra is the shifting toward higher relaxation times of the spectrum obtained from creep data; this is due to the different time intervals explored by the two approaches. Indeed, frequency test (0.01–10 Hz) investigates the time range 0.1–100 s, while creep test is carried out in the time range 1–300 s. Similar considerations can be drawn also for the other systems ( $r = 0, 0.12, \text{ and } 7$ ).

While the characterization carried out in the linear viscoelastic field provides information about the structures of our systems, the creep-recovery tests in the not linear field can provide useful information from technological point of view. Figure 9(A,B)

**Table II.** Results of eqs. (1) and (2) Best Fitting of the Frequency Sweep Data Referring to Systems Characterized by Different  $r$  Values (Some of These Data are Reported in Figure 6).

$r(-)$	0	0.12	0.5	1	2	4	7
$\overline{G^*}$	15.2	19.1	19.5	26.2	20.2	17.3	11.9
$G_1(\text{Pa})$	$13.0 \pm 1.2$	$14.0 \pm 2.5$	$21.0 \pm 11.0$	$11.3 \pm 1.7$	$14.0 \pm 8.0$	$13.0 \pm 3.0$	$11.0 \pm 2.2$
$G_2(\text{Pa})$	$8.4 \pm 0.8$	$8.2 \pm 2.0$	$9.0 \pm 3.8$	$7.2 \pm 1.5$	$10.5 \pm 3.2$	$9.3 \pm 2.3$	$7.3 \pm 2.0$
$G_3(\text{Pa})$	$7.0 \pm 0.6$	$8.2 \pm 1.7$	$9.6 \pm 2.2$	$5.8 \pm 1.2$	$8.0 \pm 2.4$	$6.6 \pm 1.8$	$4.2 \pm 1.1$
$G_4(\text{Pa})$	$5.0 \pm 0.6$	$4.3 \pm 1.6$	$6.2 \pm 1.7$	$2.4 \pm 1.8$	$5.3 \pm 1.6$	$5.1 \pm 1.6$	$4.8 \pm 1.0$
$G_5(\text{Pa})$	$8.4 \pm 0.8$	$8.4 \pm 2.2$	$8.5 \pm 2.0$	$16.0 \pm 2.2$	$4.3 \pm 2.0$	$3.2 \pm 2.1$	-
$\lambda_1(\text{s})$	$(1.2 \pm 0.4)10^{-2}$	$(1.6 \pm 0.9)10^{-2}$	$(0.4 \pm 0.2)10^{-2}$	$(2.3 \pm 0.4)10^{-2}$	$(2.0 \pm 0.3)10^{-2}$	$(2.0 \pm 0.9)10^{-2}$	$(2.5 \pm 0.8)10^{-2}$
$G(\text{Pa})$	$36 \pm 2$	$43 \pm 4$	$54 \pm 12$	$43 \pm 5$	$42 \pm 9$	$37 \pm 4$	$27 \pm 3$
$\rho_x(\text{mol}/\text{cm}^3)$	$(1.4 \pm 0.9)10^{-8}$	$(1.7 \pm 0.2)10^{-8}$	$(2.2 \pm 0.5)10^{-8}$	$(1.7 \pm 0.2)10^{-8}$	$(1.7 \pm 0.4)10^{-8}$	$(1.5 \pm 0.2)10^{-8}$	$(1.1 \pm 0.1)10^{-8}$
$\xi(\text{nm})$	$60 \pm 1$	$57 \pm 2$	$52 \pm 4$	$57 \pm 3$	$57 \pm 4$	$59 \pm 3$	$66 \pm 2$
$F$ test	$F(5, 51, 0.95)$ < 98	$F(5, 21, 0.95)$ < 21	$F(5, 21, 0.95)$ < 14	$F(5, 21, 0.95)$ < 42	$F(5, 21, 0.95)$ < 18	$F(5, 21, 0.95)$ < 16	$F(4, 21, 0.95)$ < 12

$G$  is the shear modulus, sum of the elastic contributions ( $G_i$ ) pertaining to each element of the generalized Maxwell model [eqs. (1) and (2)],  $\lambda_1$  is the relaxation time of the first Maxwell element,  $\overline{G^*}$  ( $= \sqrt{\overline{G'^2} + \overline{G''^2}}$ ) is the average complex modulus (computed resorting to the average store ( $\overline{G'}$ ) and loss ( $\overline{G''}$ ) modulus evaluated on the pulsation  $\omega$  field explored),  $\rho_x$  is the crosslink density,  $\xi$  is the average mesh size and  $F$  is the value of the  $F$  test. Fitting parameters are reported with their standard deviation

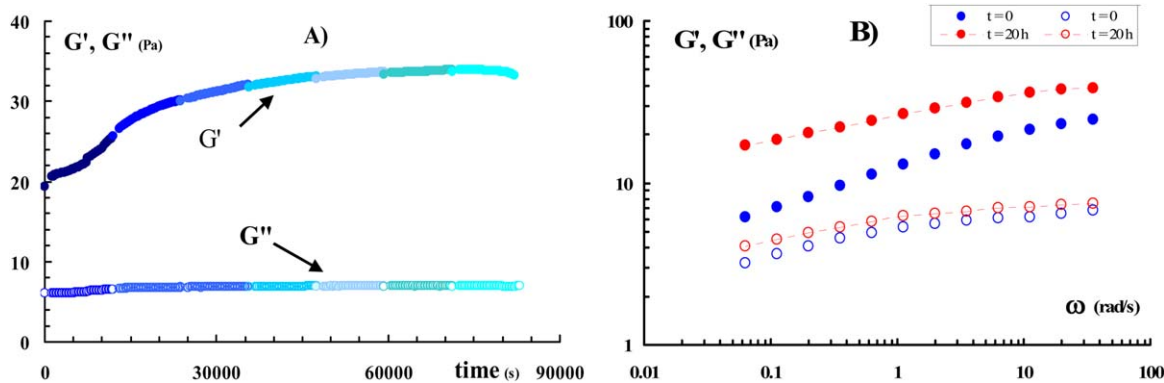


**Figure 7.** Time evolution, at 1 Hz, of  $G'$  and  $G''$  for a sample of ScIg/borax with  $r=1$  (A) and the corresponding mechanical spectra (B) recorded at  $t=0$  and  $t=20$  h ( $G'$ : full symbols;  $G''$ : open symbols;  $c_p=0.7\%$ ,  $T=25^\circ\text{C}$ ). [Color figure can be viewed in the online issue, which is available at wileyonlinelibrary.com.]

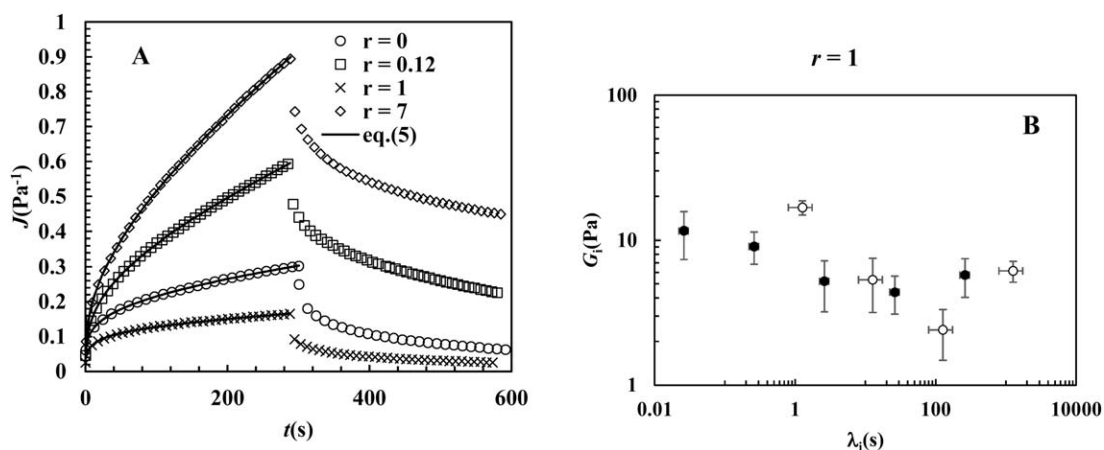


**Figure 8.** A: Creep-recovery data (symbols;  $\tau=0.1$  Pa) referring to systems characterized by different  $r$  values.  $J$  is the compliance and  $t$  is time. Continuous lines indicate eq. (5) best fitting. B: Comparison between the relaxation spectra ( $G_i$  vs.  $\lambda_i$ ) obtained by the fitting of the generalized Maxwell model to shear (filled symbols; see Table I) and creep (open symbols) data, for  $r=1$  system. Vertical and horizontal bars indicate data standard errors.

shows the trend of the compliance  $J$  vs. time  $t$  for  $r=0$  and  $r=1$  systems, respectively, when different stresses ( $\tau$ ) are applied. As expected, in both cases an increase of the applied

stress ( $\tau$ ) implies an increase of the maximum deformation. However, the difference between the two systems relies on the higher increase of deformation in the case  $r=0$ , in

**Table III.** Best Fitting of eq. (5) to Creep Data ( $\tau=0.1$  Pa) Referred to Systems Characterized by Different  $r$  Values

$r(-)$	0	0.12	1	7
$\gamma_c(-)$	0.082	0.135	0.300	0.083
$\gamma_{\max}(-)$	0.030	0.060	0.016	0.089
$G_1(\text{Pa})$	$15.4 \pm 2.9$	$17.2 \pm 0.7$	$16.7 \pm 1.9$	$13.5 \pm 0.5$
$G_2(\text{Pa})$	$5.3 \pm 0.4$	$5.0 \pm 0.3$	$5.2 \pm 2.2$	$4.0 \pm 0.3$
$G_3(\text{Pa})$	$3.6 \pm 0.5$	$2.6 \pm 0.1$	$2.4 \pm 1.0$	$2.5 \pm 0.1$
$G_4(\text{Pa})$	$2.6 \pm 0.1$	$1.9 \pm 0.1$	$6.2 \pm 1.0$	$1.1 \pm 0.1$
$G_5(\text{Pa})$	$2.3 \pm 0.6$	-	-	-
$G(\text{Pa})$	$29 \pm 3$	$27 \pm 1$	$31 \pm 3$	$21 \pm 1$
$\lambda_1(\text{s})$	$0.198 \pm 0.087$	$0.471 \pm 0.022$	$1.270 \pm 0.470$	$0.476 \pm 0.063$
$F$ test	$F(5, 94, 0.95) < 254523$	$F(4, 294, 0.95) < 463634$	$F(4, 294, 0.95) < 10051$	$F(4, 294, 0.95) < 479939$

$\gamma_c$  is the critical deformation evaluated by the frequency sweep test (see Table I),  $\gamma_{\max}$  is the maximum deformation reached in the creep experiments,  $G$  is the shear modulus, sum of the elastic contributions ( $G_i$ ) related to each element of the generalized Maxwell model [eq. (5)] and  $\lambda_1$  is the relaxation time of the first Maxwell element.



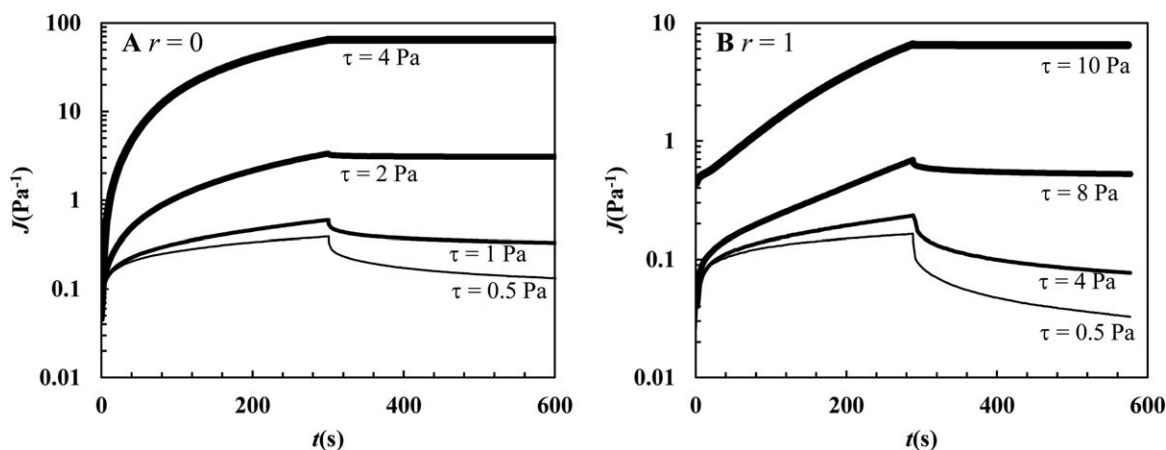


**Figure 9.** Creep-recovery data referring to system characterized by  $r=0$  (A) and  $r=1$  (B).  $J$  is the compliance,  $t$  is time and  $\tau$  is the applied stress.

comparison to the case  $r=1$ , when the same  $\tau$  is applied (e.g., when  $\tau=4$  Pa there is a difference in compliance by a factor  $\approx 10^3$ ). This, of course, is due to the different strength of the two polymeric networks. In fact, the network strength is responsible for the different fracture threshold of the two systems: for  $r=0$  and  $r=1$  the system fracture (yield stress) occurs, at  $\tau > 2$  Pa and  $\tau > 8$  Pa, respectively. Actually, when  $\tau > 2$  Pa ( $r=0$ ) and  $\tau > 8$  Pa ( $r=1$ ), the system is unable to recover, even partially, the deformation after the stress removal [see Figure 9(A,B)].

For this purpose, it is interesting to underline the effect of  $r$  on the dependence of the relative recoverable strain  $\gamma_{RS}$  on  $\tau$ :

$$\gamma_{RS} = \frac{\gamma_{MAX} - \gamma_{MIN}}{\gamma_{MAX}} \quad (6)$$

where  $\gamma_{MAX}$  is the maximum deformation of the sample (i.e., at the end of the creep phase, 300 s after the application of the stress  $\tau$ ) and  $\gamma_{MIN}$  is the system deformation at the end of the recovery period (i.e., 300 s after the stress removal). Figure 10 shows that, regardless of  $r$ ,  $\gamma_{RS}$  decreases, as expected, with  $\tau$ . However, while for  $r=0$ , 0.12, and 7 the decrease is rapid, for  $r=1$ ,  $\gamma_{RS}$  is almost constant up to  $\tau=6$  Pa and only above this

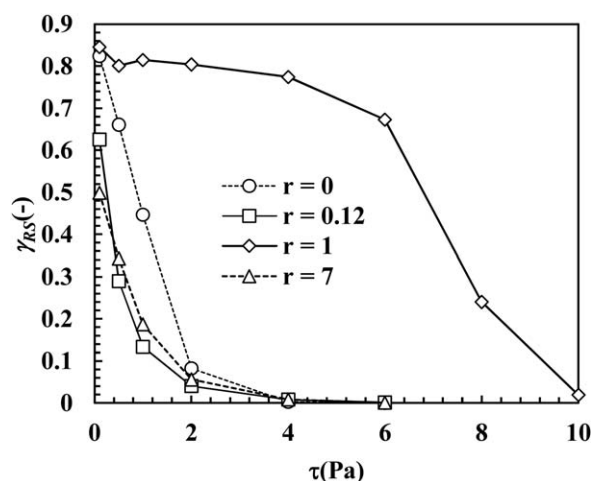


**Figure 10.** Decrease of the relative recoverable strain  $\gamma_{RS}$  on the applied stress  $\tau$  for systems characterized by different  $r$  values.

value a sharp decrease takes place. This evidence further underlines the peculiarity of the  $r=1$  system in comparisons to the other studied systems. While in linear conditions it is possible to divide the samples in two main classes (the  $r=0$ , and 7 systems from one side, and the  $r=0.12$ , 0.5, 1, 2, 4 samples from the other side), in not linear conditions the big difference arises between the  $r=1$  sample and all the other systems. This is in accordance with the fact that the  $r=1$  system shows the highest elongation upon swelling of the tablet [see Figure 3(B)].

The peculiarity of the system with  $r=1$  is to be related with the stiffness of Scg. Actually, only few linkages are enough for the formation of the gel-like system. Samples with  $0.12 \leq r \leq 2$  show similar shear moduli while the samples with  $r=0$  and 7 show lower  $G$  values (the system with an  $r$  value of 4 lies in between). In the case of Scg, where the crosslinks are absent, we observe a lower  $G$  value while for  $r=7$  the effect of electrostatic repulsions among the borate ions overcomes the “bridge-effect.” Creep experiments clearly show (Figure 10) that the strongest sample, from the mechanical point of view, is for sure that with  $r=1$ . This means that, although the number of crosslinks per unit volume is similar to that of other samples [e.g.,  $0.12 \leq r \leq 2$  ( $r \neq 1$ )], as evidenced by the similar values of shear moduli and crosslink density [see eq. (3) and Table II], the  $r=1$  sample represents the situation where the crosslinks reach their maximum effect with the best counterbalance of the electrostatic repulsion. This leads to a higher degree of the microscopic arrangement of the triple helices, as evidenced also by the swelling experiments (Figures 3 and 4). It is quite reasonable that the system with the highest structural order shows higher values of water uptake in comparison to the tablets with  $0.12 \leq r \leq 2$  ( $r \neq 1$ ), where there are more domains with entangled and clustered chains, that hinder the access of water molecules.

## CONCLUSIONS

The reported data provide a deeper insight into the physico-chemical properties of the Scg/borax hydrogel, a system, which has been considered as suitable for the formulation of modified drug delivery dosage forms.

For the first time it has been considered how different amounts of borax may influence the swelling and the rheological properties

of the hydrogel in order to better tailor the features of the system for specific needs. A visual perception, at a “microscopic” level, of the borax effect on the polymeric chains can be appreciated, for example, by means of the reported SEM images.

Furthermore, provided that borax is capable to induce a highly ordered configuration of parallel aligned bundles of Scg chains, as evidenced in previous works, the new reported results on the one-direction dimension increases of swelling tablets [see Figure 3(A,B)] indicate that, even low values of the ratio “moles of borax/moles of repeating units of polymer” ( $r = 0.02$ ) allowed the formation of a three-dimensional network. Actually, also the tablets prepared with an  $r$  value of 0.02 already show the peculiar anisotropic swelling behavior, although to a lesser extent when compared with the  $r = 1$  samples.

The rheological characterization (in the linear viscoelastic range) evidenced that there is a wide interval of borax concentrations ( $0.12 \leq r \leq 4$ ) within which the different systems show similar rheological behaviors (comparable shear moduli and crosslinking density).

In addition, the analysis of frequency sweep and creep data, performed by means of the generalized Maxwell model, correctly showed that, whichever are the considered data (frequency sweep or relaxation data), the resulting relaxation spectra were basically the same, thus proving the agreement of the two approaches. Relying on this analysis, it can be concluded that systems characterized by  $0.12 \leq r \leq 4$  share similar values of the average mesh size.

Interestingly, the characterization of our systems in the not linear viscoelastic range performed by means of creep-recovery tests, revealed the peculiarity of the  $r = 1$  system.

Indeed, this system showed the highest strength related to the not linear deformation.

This strength was evaluated determining the dependence of the recoverable strength on the applied stress in the frame of the creep-recovery tests. The peculiarity of the sample with  $r = 1$ , evidenced in the nonlinear viscoelastic range, can be related to an optimized equilibrium between the crosslinking effect of borate ions and the electrostatic repulsion.

## ACKNOWLEDGMENTS

Sapienza University Grant C26A119N2S and the Italian Ministry of Education [PRIN 2010-11 (20109PLMH2)] Grant are acknowledged.

## REFERENCES

1. Yanaki, T.; Norisuye, T. *Polym. J.* **1983**, *15*, 389.
2. Grassi, M.; Lapasin, R.; Pricl, S. *Carbohydr. Polym.* **1996**, *29*, 169.
3. Palleschi, A.; Bocchinfuso, G.; Coviello, T.; Alhaique, F. *Carbohydr. Res.* **2005**, *340*, 2154.
4. Toutilou, E.; Alhaique, F.; Ricciari, F. M.; Riccioni, G.; Santucci, E. *Drug Des. Deliv.* **1989**, *5*, 141.
5. Alhaique, F.; Carafa, M.; Ricciari, F. M.; Santucci, E.; Toutilou, E. *Pharmazie* **1993**, *48*, 432.
6. Shibayama, M.; Sato, M.; Kimura, Y.; Nomura, S. *Polymer* **1988**, *29*, 336.
7. Coviello, T.; Coluzzi, G.; Palleschi, A.; Grassi, M.; Santucci, E.; Alhaique, F. *Int. J. Biol. Macromol.* **2003**, *32*, 83.
8. Coviello, T.; Grassi, M.; Palleschi, A.; Bocchinfuso, G.; Coluzzi, G.; Banishoeib, F.; Alhaique, F. *Int. J. Pharm.* **2005**, *289*, 97.
9. Bocchinfuso, G.; Mazzuca, C.; Sandolo, C.; Margheritelli, S.; Alhaique, F.; Coviello, T.; Palleschi, A. *J. Phys. Chem. B* **2010**, *114*, 13059.
10. Coviello, T.; Bertolo, L.; Matricardi, P.; Palleschi, A.; Bocchinfuso, G.; Maras, A.; Alhaique, F. *Colloid Polym. Sci.* **2009**, *287*, 413.
11. Bocchinfuso, G.; Palleschi, A.; Mazzuca, C.; Coviello, T.; Alhaique, F.; Marletta, G. *J. Phys. Chem. B* **2008**, *112*, 6473.
12. Di Meo, C.; Coviello, T.; Matricardi, P.; Alhaique, F.; Capitani, D.; La Manna, R. *Soft Matter* **2011**, *7*, 6068.
13. Coviello, T.; Grassi, M.; Lapasin, R.; Marino, A.; Alhaique, F. *Biomaterials* **2003**, *24*, 2789.
14. Coviello, T.; Matricardi, P.; Balena, A.; Chiapperino, B.; Alhaique, F. *J. Appl. Polym. Sci.* **2010**, *115*, 3610.
15. Sandolo, C.; Coviello, T.; Matricardi, P.; Alhaique, F. *Eur. Biophys. J.* **2007**, *36*, 693.
16. Coviello, T.; Alhaique, F.; Dorigo, A.; Matricardi, P.; Grassi, M. *Eur. J. Pharm. Biopharm.* **2007**, *66*, 200.
17. Palleschi, A.; Coviello, T.; Bocchinfuso, G.; Alhaique, F. *Int. J. Pharm.* **2006**, *322*, 13.
18. Matricardi, P.; Onorati, I.; Coviello, T.; Alhaique, F. *Int. J. Pharm.* **2006**, *316*, 21.
19. Matricardi, P.; Onorati, I.; Masci, G.; Coviello, T.; Alhaique, F. *J. Drug Del. Sci. Technol.* **2007**, *17*, 193.
20. Coviello, T.; Alhaique, F.; Parisi, C.; Matricardi, P.; Bocchinfuso, G.; Grassi, M. *J. Control. Release* **2005**, *102*, 643.
21. Lapasin, R.; Pricl, S. *Rheology of Industrial Polysaccharides, Theory and Applications*; Chapman & Hall: London, UK, **1995**.
22. Kuijpers, A. J.; Engbers, G. H. M.; Feijen, J.; De Smedt, S. C.; Meyvis, T. K. L.; Demeester, J.; Krijgsveld, J.; Zaat, S. A. J.; Dankert, J. *Macromolecules* **1999**, *32*, 3325.
23. Coviello, T.; Matricardi, P.; Alhaique, F.; Farra, R.; Tesi, G.; Fiorentino, S.; Asaro, F.; Milcovich, G.; Grassi, M. *eXpress Polym. Lett.* **2013**, *7*, 733.
24. Draper, N. R.; Smith, H. *Applied Regression Analysis*; Wiley: New York, **1966**.
25. Erman, B.; Flory, P. J. *Macromolecules* **1982**, *15*, 800.
26. Erman, B.; Flory, P. J. *Macromolecules* **1982**, *15*, 806.
27. Pasut, E.; Toffanin, R.; Voinovich, D.; Pedersini, C.; Murano, E.; Grassi, M. *J. Biomed. Mater. Res. A* **2008**, *87A*, 808.
28. Gardel, M. L.; Shin, J. H.; MacKintosh, F. C.; Mahadevan, L.; Matsudaira, P.; Weitz, D. A. *Science* **2004**, *304*, 1301.
29. Schurz, J. *Progr. Polym. Sci.* **1991**, *16*, 1.
30. Li, Y.; Tanaka, T. In *Polymer Gels*; De Rossi, D. Ed.; Plenum Press: New York, **1991**; Vol. *41*, p 56.